ELSEVIER

Journal of Alloys and Compounds 404–406 (2005) 485–489

Journal of ALLOYS AND COMPOUNDS

www.elsevier.com/locate/jallcom

Microstructure of MmM_5/Mg multi-layer films prepared by magnetron sputtering

L.Z. Ouyang[a], H. Wang[a], M. Zhu[a,*], J. Zou[b], C.Y. Chung[c]

[a] *College of Mechanical Engineering, South China University of Technology, Guangzhou 510641, China*
[b] *Division of Materials and Centre for Microscopy and Microanalysis, The University of Queensland, Qld 4072, Australia*
[c] *Department of Physics and Material Science, City University of Hong Kong, 83 Tat Chee Avenue, Kowloon, Hong Kong*

Received 16 June 2004; received in revised form 5 January 2005; accepted 10 January 2005
Available online 14 July 2005

Abstract

Microstructure of $MmNi_{3.5}(CoAlMn)_{1.5}$/Mg (here Mm denotes La-rich mischmetal) multi-layer hydrogen storage thin films prepared by direct current magnetron sputtering was investigated by cross-sectional transmission electron microscopy (XTEM). It was shown that the MmM_5 layers are composed of two regions: an amorphous region with a thickness of ∼4 nm at the bottom of the layers and a randomly orientated nanocrystallite region on the top of the amorphous region and the Mg layers consist of typical columnar crystallite with their [0 0 1] direction nearly parallel to the growth direction. The mechanism for the formation of the above microstructure characteristics in the multi-layer thin films has been proposed. Based on the microstructure feature of the multi-layer films, mechanism for the apparent improvement of hydrogen absorption/desorption kinetics was discussed.

Keywords: Hydrogen storage alloys; Multi-layer films; Magnetron sputtering; Transmission electron microscopy (TEM)

1. Introduction

In past several decades, tremendous effort has been made to develop hydrogen storage alloys for its key roles in clean energy systems. Mg-base alloys have been considered as candidates with significant potentials for its high hydrogen storage capacity up to 7.6 mass%. However, hydrogenation/dehydrogenation kinetics of Mg-base alloys is generally poor and high temperature (∼573 K) is necessary for dehydrogenation process. Great effort has been made in past decades to overcome those drawbacks and substantial progress has been achieved by using different methods, such as alloying elements addition [1,2] mechanical alloying (MA) [3,4], surface modification [5] and forming non-equilibrium microstructure [6,7] including nanocrystalline and amorphous have been investigated. Recently, adding catalytic additives either by MA and film deposit method has attracted great attention. The additives added includes (i) metals and non-metals (e.g. Ce, Ti, Nb, Fe, Co, Ni, C and Si) [8–11]; (ii) mixtures of non-metal and metal [12]; (iii) 3d transition metal oxides (e.g. TiO_2, V_2O_5 and MnO_2) [13,14]; (iv) hydrogen storage alloys with superior kinetic properties [15,16]. It has been shown that the kinetics of Mg-base alloy was improved owing to the addition of catalytic additives. The improvement is enhanced by combining the nanocrystalline structure formation together with the addition of catalytic additives.

Film deposition is also an important way of synthesizing nanostructured Mg-base alloys. In the same time, catalytic additives can be incorporated into the film to form composite. Chen et al. [17] reported that an amorphous $Mg_{1.2}Ni_{1.0}$ film can absorb and desorb hydrogen under 3.3 MPa of H_2 at 150 °C. It was reported [18] that the Pd/Mg/Pd films can absorb and desorb hydrogen at 100 °C and its hydrogen storage capacity reaches to 5 mass%. However, due to the high cost of Pd, alternative catalytic components, such as rare earth alloys, are worth of consideration. The authors of the present article have reported [19] the $MmNi_{3.5}(CoAlMn)_{1.5}$/Mg (MmM_5 denote for $MmNi_{3.5}(CoAlMn)_{1.5}$ here below) multi-layer

* Corresponding author. Tel.: +86 20 87113924; fax: +86 20 87112762.
E-mail address: memzhu@scut.edu.cn (M. Zhu).

0925-8388/$ – see front matter © 2005 Elsevier B.V. All rights reserved.
doi:10.1016/j.jallcom.2005.01.120

thin films could absorb hydrogen at 473 K and desorb hydrogen completely at 523 K. It is worth emphasizing that multi-layer film is suitable for investigating the effect of microstructure and combination of components for those features can be well controlled and characterized by deposition process and microstructure analysis, respectively. The purpose of the present paper was to characterize the microstructure of MmM_5/Mg multi-layer thin films in detail by transmission electron microscopy and to explain the reason for the improvement of hydrogen absorption/desoption properties achieved in this multi-layer film system.

2. Experiments

MmM_5/Mg multi-layer thin films were deposited onto a (0 0 1) Si wafer by direct current magnetron sputtering using an Edwards Coating System (Model E306A). Two sputtering targets were used with one being MmM_5 alloy prepared by induction melting under the protection of pure argon and the other being bulk Mg with a 99.99% purity. The base pressure in the working chamber was 5×10^{-5} Pa and the working pressure in the chamber was maintained a constant value of 1.4×10^{-1} Pa during the deposition. The applied power was 250 W. The deposition rate was monitored by Edwards FTM5 thickness monitor. During the deposition process, the MmM_5 and Mg targets were alternatively sputtered to form the MmM_5 and Mg layers alternatively. Seven-layer films were prepared with the starting and finishing layers are the MmM_5.The structural and compositional investigation of cross-sectional specimens (XTEM) was carried out using a Philips CM12 TEM and a JEOL 3000F TEM equipped with an energy dispersive X-ray spectrometer (EDX). The probe size of the electron beam for performing EDX analysis could be as small as 0.5 nm in diameter.

3. Results and discussion

3.1. General morphology of the thin film

Fig. 1 is a bright field XTEM image of the MmM_5/Mg multi-layer film. It shows that the total film thickness is 3100 nm with the thickness of Mg layer and the MmM_5 layer being 500 and 400 nm, respectively. The thickness of each layer was accurately controlled and the thickness of the whole layers is homogeneous. The Mg layer and the MmM_5 layer are bonded well and the interfaces are sharp and clean. No other phases have been observed along the interface regions, implying that there was no reaction between Mg and MmM_5 during the deposition process. This is different to the situation in the process of mechanical alloying of Mg and MmM_5, where a solid-state reaction takes place between Mg and MmM_5. However, careful observation of the interface shows that the interfaces are not awfully flat and small fluctuation, which is indicated by the arrow in figure, exist along

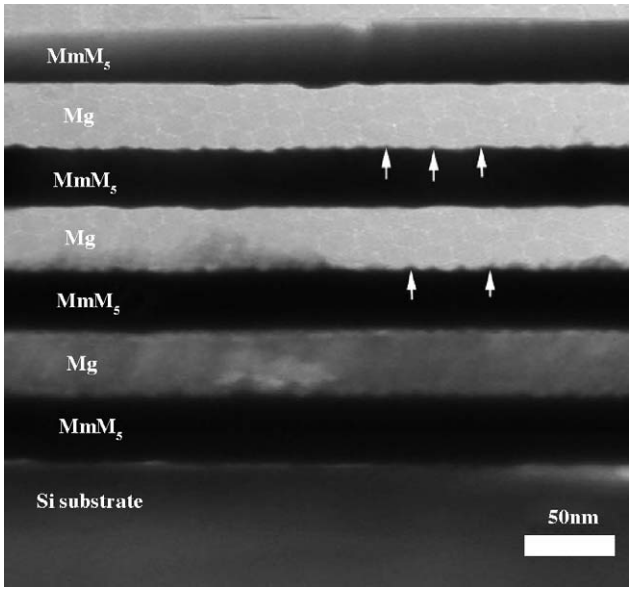

Fig. 1. XTEM image of the MmM_5/Mg multi-layers film obtained by magnetron sputtering.

interfaces. Detail TEM and HRTEM observations described below show that the Mg layer and the MmM_5 layer have their own specific microstructure feature.

3.2. Microstructure of the MmM_5 layer

The MmM_5 layers in the multi-layer film were grown on two different bases: one is on the single crystal (0 0 1) Si wafer and the other is on the as-deposited Mg layer. HRTEM observation shows that the microstructure of the MmM_5 layer deposited on Si base and Mg base is not apparently different. Fig. 2 shows the interface region between the MmM_5 layer and the Mg layer. As demonstrated in Fig. 2(a), a thin amorphous layer about 4 nm thick is on the Mg layer. EDX analysis of the thin amorphous layer proved its composition being consistent with the MmM_5 alloy, meaning that the amorphous was initially formed during the deposition of the MmM_5 layer on the Mg layer. With further growth, the amorphous phase changes to a crystalline phase. The electron diffraction pattern taken from the crystalline region is inserted in the up-left corner of Fig. 2. Indexing of the electron diffraction pattern confirms that the crystalline phase has the $CaCu_5$ structure. The continuity of the diffraction halos reveals that the grain size of the crystalline phase is rather small and they have been estimated to be about 3–10 nm using HRTEM. Our extensive TEM investigation suggests that, once the nanocrystalline grains are formed, the rest of the MmM_5 growth would keep this fashion to the end of the layer growth.

As well known, amorphous MmM_5 is easily formed when it is rapidly solidified. It is noted in the present case that the Mg layer was completely cold before the deposition process because that there is an interrupt between the depositing of different layers and the substrate was cooled by the cyclic

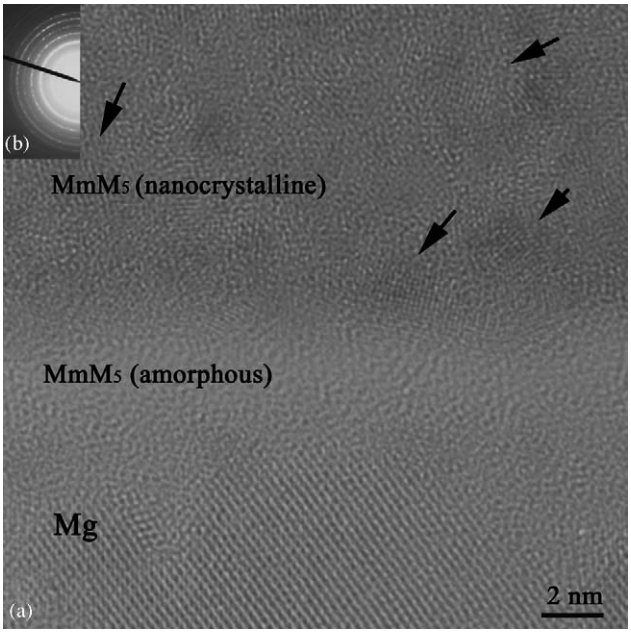

Fig. 2. HRTEM image of MmM_5 layers deposited on the as-deposited Mg layer with the SADP inserted on the up-left corner. The SADP corresponds to $CaCu_5$ structure.

water throughout the deposition process. When the growth of the Mg layer was finished and before the growth of the MmM_5 layer was started, the temperature of the substrate was decreased during the interrupt. As a result, the deposited material should experience a rapid cooling and consequently form an amorphous layer at the initial stage of the deposition of the MmM_5 film. With further growth of the MmM_5 film, the substrate has become warm due to the non-stead thermal state processing condition and the initially formed amorphous layer also acting as a thermal barrier to the substrate cooling. Therefore, the formation of the crystalline MmM_5 phase could not be suppressed and crystalline MmM_5 nuclei is formed on the surface of the amorphous layer. Since the cooling rate in the deposition process is rather high, the nucleation rate of the crystalline phase is high and its growth rate is low. Furthermore, the complicated composition of the MmM_5 alloy makes the atomic re-configuration difficult to take place, because a long-range diffusion is needed for the growth of a crystalline phase. Therefore, MmM_5 crystal nuclei formed in the MmM_5 layer is difficult to grow, and consequently, nanocrystalline structure is formed. The fact that the microstructure of the MmM_5 layer deposited on the top of the Mg layer is the same as that deposited on the Si substrate reveals that the microstructure of the deposited MmM_5 layer is mainly dependent upon the substrate temperature, regardless of the nature of the substrate, such as composition and structure.

3.3. The Mg layer deposited onto the MmM_5 layer

Fig. 3(a and b) shows the bright field and the dark field images taken from a Mg layer deposited on the top of MmM_5

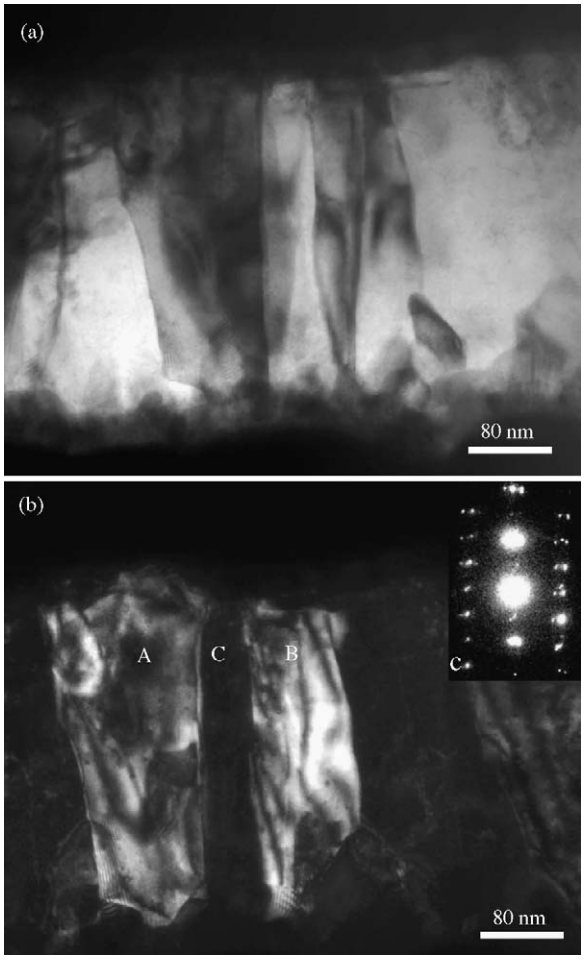

Fig. 3. TEM images of the Mg layers showing the columnar crystal: (a) bright field image, (b) dark field image and (c) composite electron diffraction pattern of three columnar Mg crystals.

layer, showing clearly that the Mg layer is composed of two regions: one is a randomly orientated nanocrystalline region of about 50 nm thick formed at the bottom of Mg layer, implying that, at the beginning of the Mg layer growth on top of the MmM_5 layer, nanocrystalline Mg is formed and the rest of the Mg layer is bundles of nearly parallelled columnar Mg crystallites with the width of about 100 nm. The long axis direction of the columnar crystal is parallel to the [0 0 1] orientation of the Mg. It means that the growth direction of Mg crystals is [0 0 1].

Although large-angle grain boundaries between columnar crystallites can also be observed occasionally, the [0 0 1] orientations of columnar crystallites are generally randomly deviated from each other in a range of small angles in most cases. Fig. 3(c) is a composite electron diffraction pattern of three columnar crystals. [0 0 1] diffraction patterns of all the three crystals can be seen but they are not coincident. This means that those three columnar crystals are not in strictly the same orientation. The orientation between neighboring columnar crystals was estimated by nanobeam electron diffraction. Many measurements have been made and the

experiment shows that orientation difference is less than 10°. For example, the angle between the (0 0 1) planes of the two columnar crystallites, as indicated by A and B, in Fig. 3(b), is about 5°. It should be mentioned that the grain boundary is not a symmetric tilted type in all the cases observed. Therefore, it is impossible to obtain a clear HRTEM image of the boundary of the two neighboring crystallites while keep the (0 0 1) planes of the both crystallites parallel to the incident electron beam.

3.4. Mechanism for the improvement of hydrogen absorption kinetic in the Mg/MmM_5 multi-layer film

Since the amount of the film obtained in this work is small and very difficult to peel off from the substrate, it is difficult to make PCI measurements for the as prepared film. However, the hydriding/dehydriding of the MmM_5/Mg multi-layer thin films can be preliminarily examined by measuring the XRD pattern of the film when subjected to hydrogenation and dehydrogenation under different conditions. Fig. 4(a–c) is XRD pattern of MmM_5/Mg multi-layer thin film after hydrogenation under 2 MPa at 200 and 250 °C for 2 h and dehydrogenation at 250 °C for 1 h. As shown in Fig. 4(a), diffraction peaks of both Mg and MgH_2 appear in the XRD patterns, which indicate that part of the Mg in the film was hydrogenated at 200 °C. The relative intensity of the MgH_2 peaks in Fig. 4(b) is much stronger than that in Fig. 4(a) and the peak intensity of Mg is very small. This result means that most of Mg was hydrogenated at the temperature of 250 °C. But the hydrogenation of Mg film was still not fully completed at 250 °C. It should also be pointed out that no apparent peak of MgH_2 was observed when hydrogenation temperature was below 150 °C. Fig. 4(c) is the XRD pattern of the MmM_5/Mg multi-layer thin film after dehydrogenation at 250 °C for 1 h. There is no MgH_2 peak left and only Mg peaks are observed, which shows that MgH_2 could completely decompose under these conditions. Comparing Fig. 4(b) and (c), it is noted

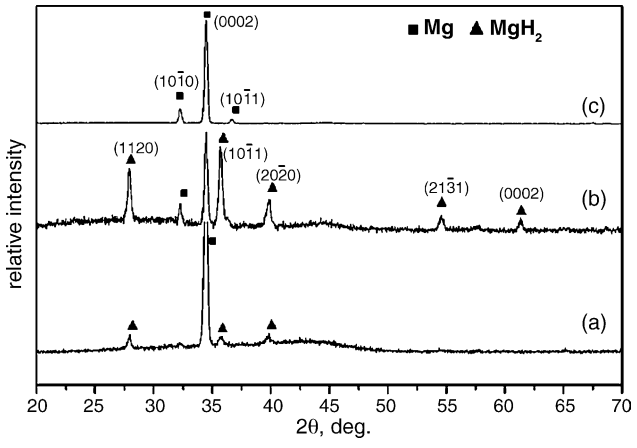

Fig. 4. XRD patterns of MmM_5/Mg multi-layer thin film (a) after hydrogenation under 2 MPa at 200 °C for 2 h, (b) after hydrogenation under 2 MPa at 250 °C for 2 h and (c) dehydrogenation at 250 °C for 1 h.

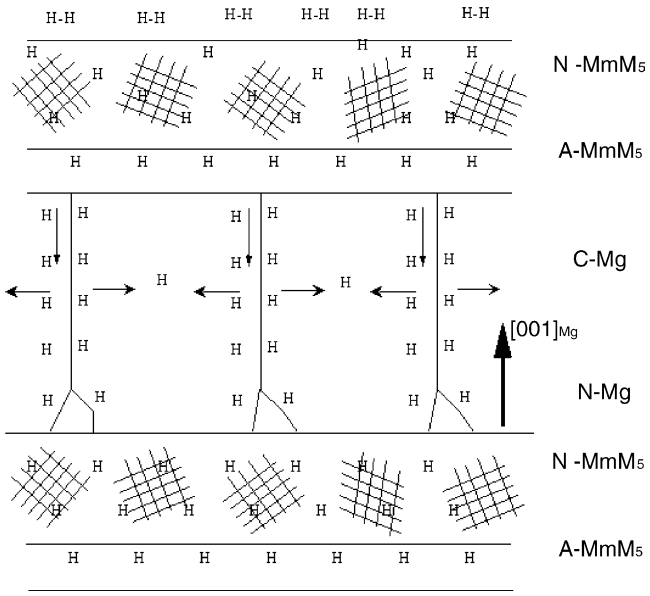

Fig. 5. Schematic diagram of hydrogenation process of MmM_5/Mg multi-layer films: N-MmM_5, A-MmM_5, C-Mg and N-Mg indicate for nanocrystalline MmM_5, amorphous MmM_5, columnar Mg crystallites and nanocrystalline Mg, respectively.

that the (1 0 $\bar{1}$ 3) peak of Mg in the XRD patterns of the as-deposited film has disappeared and the (1 0 $\bar{1}$ 0) and (1 0 $\bar{1}$ 1) diffraction peaks of Mg have appeared after hydrogenation and dehydrogenation process. This result implies that recrystallization of the as-deposited Mg crystalline microstructure took place after the hydrogenation and dehydrogenation process.

The improvement in kinetic properties must be related to the microstructure feature of the multi-layer film. A possible mechanism for the improvement of hydrogen absorption/desorption has been proposed as the schematic illustration given in Fig. 5. When the film is ready to absorb hydrogen, the MmM_5 layer on the surface of the film easily absorbs hydrogen for the hydrogen absorption kinetic of MmM_5 is very good. Then, the Mg adjacent to the MmM_5 layer should be easily hydrogenated because that the MmM_5 phase may catalyze the hydrogenation reaction of Mg in mechanism of autocatalysis [15] or “cooperative phenomena” [7]. On the other hand, the boundaries between the columnar crystallites of Mg provide many fast diffusion channels for hydrogen to diffuse into the interior of the Mg layer. Furthermore, the diffusion channels give the gateway through which hydrogen could diffuse along the substrate plane of Mg, close packed (0 0 1) plane, thus avoiding the hydrogen to diffuse through the closest packed plane of magnesium. Therefore, the hydrogenation kinetics of Mg could be improved. Vice verse, the dehydrogenation reaction is the reverse process of hydrogenation. The mechanism of improving diffusion and reaction kinetics described above is still valid. It is interesting to note that, in this experiment, no thin film was peeled off from the substrate after hydro-

genation and dehydrogenation cycles. This implies that the strain along the direction parallel to the substrate plane is not very high, which might be related to the columnar structure of the Mg film, and the bonding between substrate and the film is good.

4. Summary

It has been demonstrated that high quality Mg/MmM_5 multi-layer composite films can be prepared by direct current magnetron sputtering with well controlled film thickness and well bonded interface between different layers. Apparently, the microstructures of the MmM_5 layer and the Mg layer are different. For the MmM_5 layer, the majority is MmM_5 nanocrystallites with a thin layer of amorphous ($\sim$4 nm) appeared at the bottom of the layer. For the Mg layer, the majority is columnar crystallites with a thin layer of randomly orientated nanocrystallites ($\sim$50 nm in size) at the bottom of the layer. Most of columnar crystallites have their [0 0 1] directions roughly parallel to the growth direction. All interfaces between different layers are clean without interface phases. The formation of the film microstructure is mainly dependent on the deposition conditions and the composition of the deposited layer. The microstructure feature of the multi-layer film is a key role for understanding the mechanism of improving hydrogen absorption/desorption kinetics of Mg-base alloys.

Acknowledgements

The project was supported by National Natural Science Foundation of China under Grant Nos. 50131040 and 50401015 and by Ministry of Science and Technology of China under Grant No. 2002CCA02300.

References

[1] J.-L. Bobet, E. Akiba, Y. Nakamura, B. Darriet, Int. J. Hydrogen Energy 25 (2000) 987.
[2] A. Zaluska, L. Zaluski, J.O. Ström-Olsen, Appl. Phys. a 72 (2001) 157.
[3] N. Cui, P. He, J.L. Luo, Acta Mater. 47 (1999) 3737.
[4] M. Zhu, Z.M. Wang, C.H. Peng, M.Q. Zeng, Y. Gao, J. Alloys Compd. 349 (2003) 284.
[5] Q.M. Yang, M. Ciureanu, D.H. Ryan, J. Alloys Compd. 274 (1998) 266.
[6] J. Huot, G. Liang, R. Schulz, J. Alloys Compd. 353 (2003) 112.
[7] S. Orimo, H. Fujii, Appl. Phys. a 72 (2001) 167.
[8] Z. Dehouche, J. Goyette, T.K. Bose, R. Schulz, Int. J. Hydrogen Energy 28 (2003) 983–988.
[9] O. Gutfleisch, N. Schlorke-de Boer, N. Ismail, M. Herrich, A. Walton, J. Speight, I.R. Harris, A.S. Pratt, A. Züttel, J. Alloys Compd. 356–357 (11) (2003) 598–602.
[10] H. Imamura, N. Sakasai, T. Fujinaga, J. Alloys Compd. 253–254 (20) (1997) 34–37.
[11] H. Imamura, N. Sakasai, J. Alloys Compd. 231 (15) (1995) 810–814.
[12] G. Barkhordarian, T. Klassen, R. Bormann, Scripta Mater. 49 (2003) 213–217.
[13] Z. Dehouche, T. Klassen, W. Oelerich, J. Goyette, T.K. Bose, R. Schulz, J. Alloys Compd. 347 (1–2) (2002) 319–323.
[14] D.S. Lee, I.H. Kwon, J. Bobet, M.Y. Song, J. Alloys Compd. 366 (10) (2004) 279–288.
[15] M. Zhu, Y. Gao, X.Z. Che, Y.Q. Yang, C.Y. Chung, J. Alloys Compd. 330–332 (17) (2002) 708–713.
[16] G. Liang, J. Huot, S. Boily, A. Van Neste, R. Schulz, J. Alloys Compd. 297 (1–2) (2000) 261–265.
[17] J. Chen, H. Yang, Y. Xia, N. Kuriyama, Q. Xu, T. Sakai, Chem. Mater. 14 (2002) 2834.
[18] K. Higuchi, K. Yamamoto, H. Kajioka, K. Toiyama, M. Honda, S. Orimo, H. Fujii, J. Alloys Compd. 330–332 (2002) 526.
[19] H. Wang, L.Z. Ouyang, C.H. Peng, M.Q. Zeng, C.Y. Chung, M. Zhu, J. Alloys Compd. 370 (2004) L4.